PHILOSOPHICAL TRANSACTIONS OF THE ROYAL SOCIETY A MATHEMATICAL, PHYSICAL & ENGINEERING SCIENCES

The Lattice Thermal Conductivity of Silver Alloys between 0 $\cdot $3 and 4 degrees K

M. H. Jericho

Phil. Trans. R. Soc. Lond. A 1965 **257**, 385-407
doi: 10.1098/rsta.1965.0010

THE LATTICE THERMAL CONDUCTIVITY OF SILVER ALLOYS BETWEEN 0·3 AND 4 °K

By M. H. JERICHO*

Cavendish Laboratory, University of Cambridge

(*Communicated by A. B. Pippard, F.R.S.—Received* 1 *June* 1964)

CONTENTS

The thermal and electrical conductivities of silver and copper alloys with high electrical resistivities were studied in the temperature range from 0·3 to 4 °K. The lattice thermal conductivity results were interpreted in terms of Pippard's semi-classical theory of the electron-phonon interaction and good qualitative agreement between this theory and the measurements was obtained for the temperature range from 1 to 4 °K. Below 1 °K the thermal conductivity of most samples decreased much more rapidly than one would have expected if the phonon mean free path were limited by the electron-phonon interaction only. Other phonon scattering mechanisms were therefore postulated and the effects of phonon scattering from dislocations was studied both theoretically and experimentally. The increase in thermal resistance below 1 °K of most alloys was more rapid than the increase obtained theoretically for phonon-dislocation and phonon-boundary scattering. The thermal conductivity of a copper sample with a resistance ratio of about 85 was found to be anomalous below 1 °K as well, suggesting that both the phonons and the conduction electrons could contribute to the effect in the alloys.

1. Introduction

The standard treatment of the electron-phonon interaction as reviewed by Klemens (1958) leads to a quadratic temperature dependence of the lattice thermal conductivity of dilute alloys. Since the attenuation coefficient for a phonon of wavenumber q is a measure of its scattering or absorption probability, Pippard (1957) argued from his semi-classical theory of the ultrasonic attenuation that the lattice conductivity would be proportional to T^2 only when $ql > 1$, where l is the electron mean free path, but change over to a linear temperature dependence when $ql < 1$. The lattice thermal conductivity would therefore be represented approximately by the equation

$$K_g = AT + BT^2.$$

* Present address: Department of Physics, Dalhousie University, Halifax, Nova Scotia.

Vol. 257. A. (Price 9*s*.; U.S. $1.35) 48 [Published 25 March 1965

The existence of this linear term was first demonstrated by Zimmerman (1959) who measured the lattice thermal conductivity of a series of silver-antimony alloys in the liquid helium range of temperatures.

The importance of the transverse modes for the heat transport was pointed out by Olsen (1960), and later Lindenfeld & Pennebaker (1962) used the complete expressions for both the longitudinal and transverse sound wave attenuation and calculated the lattice thermal conductivity of alloys for the free electron model. The overall features of these theoretical curves were reproduced fairly well by their experimental conductivity curves for a number of copper-germanium alloys and they were thus able to demonstrate the important part that the transverse polarization branches play in the heat transport. In order to obtain a more rigorous test of the theory, however, it is desirable to extend the lattice thermal conductivity measurements to lower temperatures so that the parameter ql for the dominant phonons can be taken unambiguously from $ql > 1$ to $ql < 1$ with a single sample. The weakening of the electron-phonon interaction as the electron mean free path becomes short compared to the phonon wavelength should then be more readily observable.

The electrical and thermal conductivities of a number of silver-antimony and silver-tin alloys, all of which were α-phase solid solutions, were therefore measured in a helium-3 cryostat. In addition, a few copper alloys were investigated in order to obtain information about the effect of the solvent type on the low temperature lattice conductivity.

2. Theoretical discussion

In non-superconducting alloys both the conduction electrons and the lattice vibrations are of importance for the heat transport. The most common method for separating these two contributions is to take recourse to the Wiedemann–Franz law which was shown by Chester & Thellung (1961) to hold for a non-interacting electron assembly and in the presence of purely elastic scattering irrespective of the strength of the scattering.

The theoretical calculation of the lattice thermal conductivity is considerably more difficult than the calculation of the electronic part in view of the large number of phonon scattering mechanisms which can limit the heat transport. Fairly successful interpretations of heat conductivity data on insulators and semiconductors have been possible, however, with Callaway's (1959) model for the lattice conductivity.

In well-annealed alloys and in the liquid helium range of temperatures the phonon mean free path should be limited mainly by the electron-phonon interaction. The strength of this interaction can be calculated, when the phonon wavelength is considerably larger than the lattice spacing, from a theory of the ultrasonic attenuation in metals, since the reciprocal of the attenuation coefficient $\alpha(q)$, is a measure of the mean free path of a phonon with wave vector q. A quite general expression for the attenuation coefficient of a high frequency sound wave has been derived by Pippard (1960). His expression for the attenuation coefficient in its most general form is

$$\alpha = \frac{\hbar q}{4\pi^3 v_s d}\left\{\int \frac{D^2 a\, \mathrm{d}s}{1+a^2\cos^2\phi} + \frac{e^2\rho_{ij} I_i I_j}{4\pi^3\hbar q}\right\}, \tag{1}$$

where ρ_{ij} is the resistivity tensor and where

$$I_i = \int a_i \left(\frac{Da\cos\phi}{1+a^2\cos^2\phi}\right) \mathrm{d}s. \tag{2}$$

The other parameters that enter into expression (1) are: q, phonon wavenumber; d, density of the metal; v_s, sound velocity; $\mathbf{l}$, electron mean free path, considered as a vector parallel to the electron velocity; $\mathbf{a} = q\mathbf{l}$. ϕ is the angle which the electron velocity vector makes with the direction of sound propagation. The integration is performed over the Fermi surface.

The quantity D in effect measures the deformation of the local Fermi surface when a moving strain field such as an acoustic wave exists in a metal. D will in general be a complicated function of position on the Fermi surface as well as of the sound polarization and it can in practice only be specified exactly for a spherical Fermi surface.

It is not immediately obvious that this theory of ultrasonic attenuation is applicable up to low-temperature phonon frequencies ($\sim 10^{11}$ c/s). Even though the parameter ql can have the same range of values in an alloy at low temperatures as is normally obtained in ultrasonic experiments, the quantity δ/λ—where δ is the skin depth for electromagnetic waves and λ the phonon wavelength—does not scale.

In an alloy at low temperature δ/λ is always much larger than unity so that screening of the ion currents for transverse waves will always break down. The effect of the breakdown of screening on the attenuation coefficient has been considered by Pippard (1962) and the result is that in the high frequency limit when $\delta/\lambda \gg 1$ the second term in equation (1) is negligible so that the attenuation expression for longitudinal and transverse vibrations have identical form and are given by

$$\alpha_{l,t} = \frac{\hbar q}{4\pi^3 v_s d}\left\{\int \frac{D^2 a\,\mathrm{d}s}{1+a^2\cos^2\phi}\right\}. \tag{3}$$

When $a = ql \ll 1$ equation (3) reduces to

$$\alpha_{l,t} = \frac{\hbar q^2}{4\pi^3 v_s d}\int D^2 l\,\mathrm{d}s.$$

In this limit the attenuation for both the longitudinal and transverse vibrations has therefore a quadratic wavenumber dependence. The average phonon energy at low temperatures is of order $k_B T$ and in the liquid helium range of temperatures the lattice specific heat will vary as T^3. From the simple kinetic expression for the thermal conductivity it then follows that the lattice conductivity could be expected to be proportional to the absolute temperature.

In the opposite extreme when $ql \gg 1$ the wavenumber dependence of the attenuation will depend on the detailed behaviour of D. When $ql \gg 1$ the only electrons which can interact effectively with the sound wave are those that travel nearly at right angles to the direction of sound propagation and which are contained in a strip on the Fermi surface of width $1/ql$, called the effective zone. In this limit, then, and for a non-vanishing D on the effective zone the attenuation can be written quite generally as

$$\alpha_{l,t} = \frac{\hbar q}{4\pi^3 v_s d}\oint RD^2\,\mathrm{d}\psi, \tag{4}$$

where R is the Gaussian radius of curvature of the Fermi surface and the integration is performed around the effective zone. The attenuation is therefore proportional to q for both the longitudinal and transverse branches.

In order to obtain somewhat more quantitative results it is necessary to consider the free electron model since only for this case can D be specified exactly.

PHILOSOPHICAL TRANSACTIONS OF THE ROYAL SOCIETY A MATHEMATICAL, PHYSICAL & ENGINEERING SCIENCES

The complete analytic expressions for the attenuation in this case of a free electron model together with their limiting forms when $ql \gg 1$ are

$$\left.\begin{aligned} \alpha_l &= \frac{Nm}{v_l d\tau}\left\{\frac{1}{3}\frac{a^2\tan^{-1}a}{a-\tan^{-1}a}-1\right\} \\ \text{and}\quad \alpha_l &\to \frac{\pi Nm v_F q}{6 v_s d} \quad \text{when} \quad ql \gg 1; \end{aligned}\right\} \tag{5}$$

$$\left.\begin{aligned} \alpha_t &= \frac{Nm}{v_t d\tau}\left\{1-\frac{3}{2a^3}\left(\frac{(a^2+1)\tan^{-1}a}{a}-1\right)\right\} \\ \text{and}\quad \alpha_t &\to \frac{Nm}{v_t d l} \quad \text{when} \quad ql \gg 1. \end{aligned}\right\} \tag{6}$$

In these expressions N is the number of electrons per unit volume, m the electron mass and τ the electron relaxation time.

The limiting form of expression (6) is quite different from expression (4) in that the free electron model gives a frequency independent attenuation when $ql \gg 1$ and when screening is incomplete.

When the phonon frequency is high, such that $ql \gg 1$ but still low enough so that screening in the metal is complete, then the transverse sound attenuation expression for the free electron model is very similar to that for longitudinal sound (equation (5)) and is given by

$$\left.\begin{aligned} \alpha_t &= \frac{2Nma^3}{3v_t d\tau}\{[a^2+1]\tan^{-1}a-a\}^{-1}, \\ \text{and}\quad \alpha_t &\to \frac{4}{3}\frac{Nmv_F q}{\pi v_t d} \quad \text{when} \quad ql \gg 1. \end{aligned}\right\} \tag{7}$$

The reciprocals of these attenuation coefficients then define a phonon mean free path and substitution into Callaway's thermal conductivity expression,

$$K_g = \frac{1}{3(2\pi^2)}\sum_{\epsilon}\int \frac{k_B^4 T^3}{\hbar^3 v_\epsilon^3}\Lambda_\epsilon(x)\frac{x^4 e^x dx}{(e^x-1)^2}, \tag{8}$$

enables one to calculate the separate contributions to the lattice conductivity of the longitudinal and transverse lattice vibrations.

The parameters that appear in expression (8) are: $\Lambda_\epsilon(x)$, effective phonon mean free path; v_ϵ, sound velocity; k_B, Boltzmann constant; ϵ, phonon polarization vector; $x = \hbar\omega/k_B T$; T = absolute temperature.

Such calculations were first made by Zimmerman (1959) for the longitudinal modes in silver base alloys, and later Lindenfeld & Pennebaker (1962) evaluated the separate contributions of the longitudinal and transverse modes for copper base alloys using the free electron equations (5) and (6). Numerical thermal conductivity calculations for silver base alloys have now been made along essentially the same lines as the calculations of Lindenfeld & Pennebaker and it was again assumed that the two polarization branches can be treated independently. The results of this calculation are given in figure 1 which shows that the lattice conductivity divided by the absolute temperature and the residual resistivity, ρ_0, is a universal function of the parameter T/ρ_0 (or its equivalent, ql).

The characteristic features of these curves are the quadratic or higher power temperature dependence of the lattice conductivity for large T/ρ_0 values and the approach to a linear temperature dependence when T/ρ_0 is small or the electron mean free path short compared to the average phonon wavelength. Furthermore, this approach to a linear temperature dependence of the lattice conductivity should be independent of the Fermi surface shape and other details of the model.

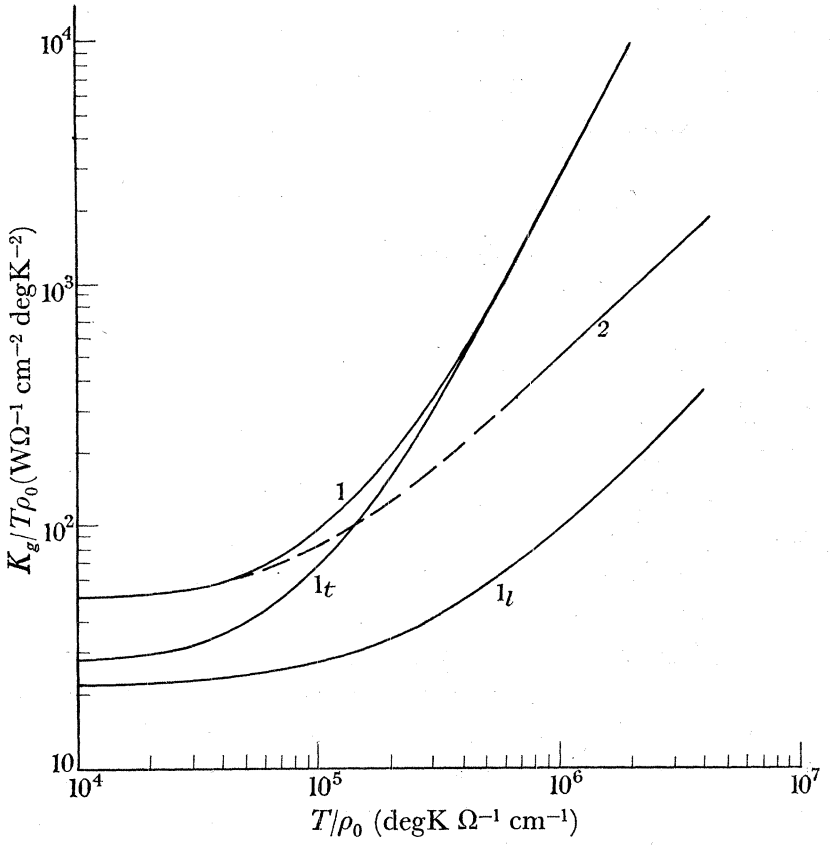

$v_l = 3{\cdot}65 \times 10^5$ cm/s; $v_t = 1{\cdot}61 \times 10^5$ cm/s; $1/\rho_0 l = 8{\cdot}38 \times 10^{-12}$(c.g.s.).

FIGURE 1. Reduced lattice conductivity curves for silver alloys: curves 1, 1_l and 1_t are the theoretical curves for the free electron model; curve 2 represents a possible variation of $K_g/T\rho_0$ for a non-spherical Fermi surface.

The contribution of the transverse modes to the heat transport in the limit $ql \gg 1$ is, however, dependent on the model as a comparison of equations (4) and (6) show. For the non-spherical Fermi surface in silver the attenuation will most likely follow expression (4). Both polarization branches will then have attenuation coefficients proportional to the wavenumber and both branches could be expected to give rise to a conductivity that varies as T^2. In order to obtain some qualitative information about the size of the upward curvature that could be expected in the thermal conductivity of these alloys in the temperature range between 0·3 and 4 °K the transverse sound attenuation in the limit $ql \gg 1$ was taken to be given by equation (7). Substitution of the corresponding phonon mean free path into equation (8) then gives a qualitative estimate of the transverse phonon contribution to the heat transport, and addition of the contribution of the longitudinal branch (curve 1_l) resulted in the upper solid section of curve 2 in figure 1. This section must then eventually

join on to the lower section of curve 1 and the behaviour in the intermediate region was assumed to be given by the dashed portion of curve 2. This second theoretical curve gives a much smaller curvature effect when K/T is plotted as function of T than curve 1 for the free electron model. In particular, an experimental error of 2% could easily mask the curvature in the liquid helium-4 range of temperatures, although the deviations from a straight-line relationship should become easily measurable below 1 °K. It must be emphasized, however, that the total lattice conductivity curve 2 of figure 1 gives only a qualitative description of the expected lattice conductivity of an alloy with a non-spherical Fermi surface. That is, it probably gives the correct temperature dependence in the region where $ql \gg 1$, but nothing can be said about the absolute magnitude of the conductivity.

3. Experimental technique

(*a*) *Cryostat*

In order to test the theoretical predictions of § 2 it is desirable to measure the thermal conductivity of a given alloy specimen over as wide a range of low temperatures as possible, so that a reasonably long portion of the theoretical curves in figure 1 can be traced out with a single sample. The thermal and electrical conductivity measurements were therefore made in a helium-3 cryostat.

The main feature of the cryostat was the use of a four-stage mercury diffusion pump (Speedivac pump 2M4-A) for the vapour-pressure reduction of the helium-3 bath. This pump requires a backing pressure of about 35 mmHg. The vapour pressure of helium-3 at 1·2 °K is about 25 mmHg so that a small helium-3 gas recondenser situated in the helium-4 bath at that temperature could act as a backing pump for the 2M4-A. This was an extremely convenient arrangement and provided a very compact closed-circuit helium-3 system. The helium-3 gas recovery was performed by an automatic mercury Toepler pump.

Details of the low-temperature stage are shown in figures 2*a* and 2*b*. The helium-3 vessel was constructed from copper and had a capacity of 2·5 cm^3. A set of concentric grooves were cut into its base in order to increase the effective contact area and improve the heat exchange between the helium-3 bath and specimen holder. The helium-3 vessel was connected to the top plate of the outer can through Cu-Ni tubes of 0·2 mm wall thickness. The tube for the helium-3 pumping line was 13 cm long and 6 mm in diameter and contained a radiation trap which was situated close to the top plate of the outer can. Heat transfer in the initial cool down between the helium-4 bath and the helium-3 vessel and salt thermometer was achieved through the use of helium-4 as an exchange gas between the outer can and the inner can. The exchange gas cooled the top plate (H) and a copper tube (C) surrounding the helium-3 pumping line provided a good thermal path between the top plate and the helium-3 vessel. All electrical leads were brought down inside the sample space pumping tube (B) and were thermally anchored to the helium-4 bath as well as the helium-3 vessel. All leads were made from no. 42 s.w.g. enamelled Eureka wire.

(*b*) *Salt thermometer*

An ellipsoid of a single crystal of cerium magnesium nitrate was used for the absolute temperature measurements below 1·5 °K. The salt tube (G) as well as the lower sections of the two cans were constructed from phosphor-bronze tubing of 0·2 mm wall thickness.

All joints were hard soldered so that the nearest superconducting material was at the sample receptor (R).

The salt tube was filled with helium-4 gas at liquid nitrogen temperature and the gas pressure was adjusted to be one atmosphere at room temperature. This form of heat contact,

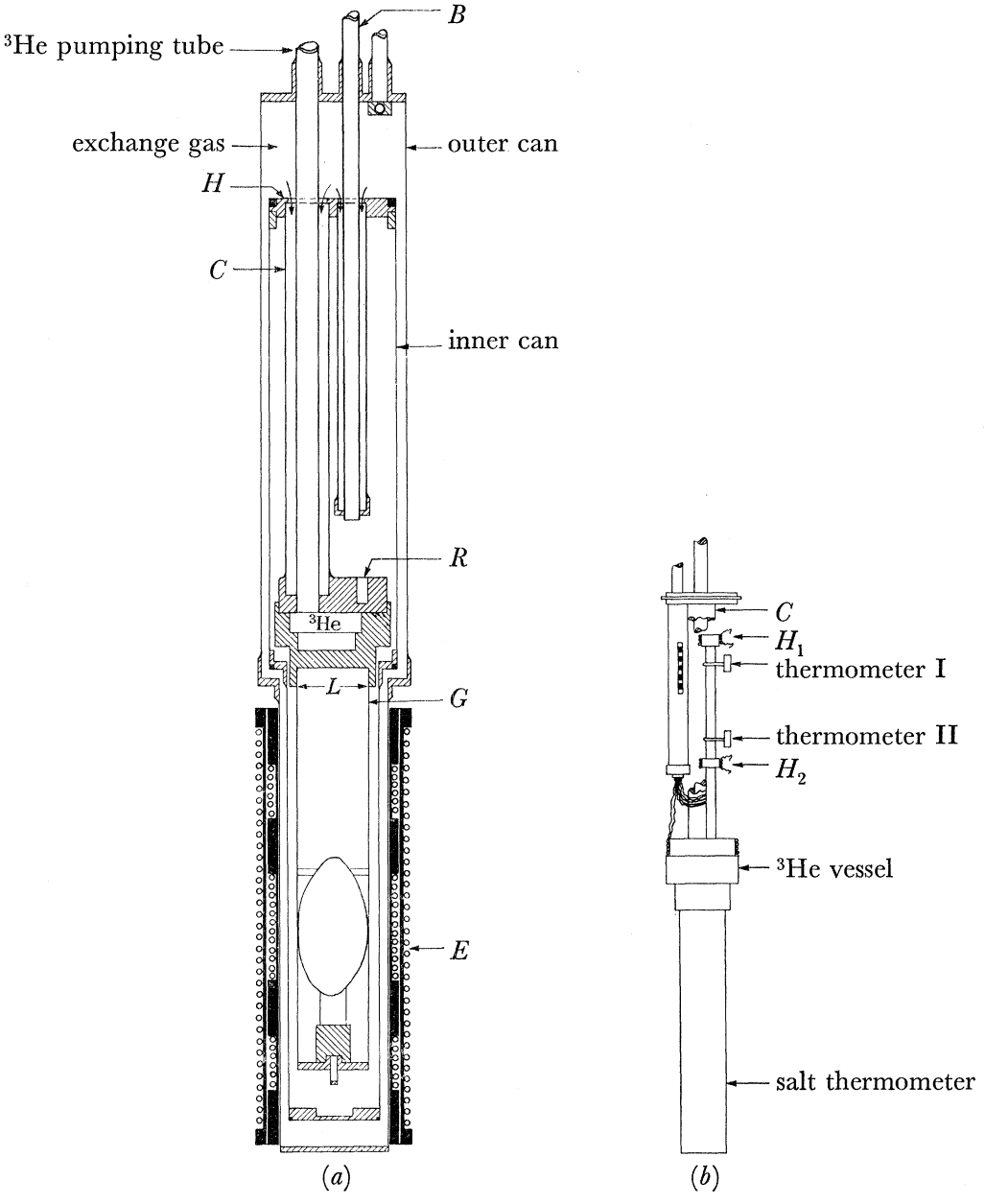

FIGURE 2. The specimen assembly.

described previously by Seidel & Keesom (1958), proved very effective although around 0·5 °K the thermal conductivity of a superfluid helium film was smaller than that of phosphor-bronze so that the former provided a thermal link only between the salt pill and the can surface directly opposite to it.

In order to protect the salt from the direct heat when the last joint at L was made during assembly about 1 g of Pyrex glass wool was inserted into the space above the salt.

The susceptibility of the salt was measured with an a.c. mutual inductance bridge of the Hartshorne type and was operated at a frequency of 37 c/s. The signal source was a tuning fork oscillator, and a high gain selective amplifier together with a phase-sensitive detector served as null indicator. The primary and secondary of the susceptibility coils (E) were wound on separate formers with the secondary fitting closely into the primary coil. The secondary coil was wound in three sections in an astatic manner and measurements were made with a field at the salt pill of approximately 1 G.

Both the helium-4 and the helium-3 baths were temperature-stabilized. The helium-4 bath was stabilized to better than 10^{-3} degK with an Adkins (1961) liquid helium bath stabilizer. Temperature stabilization of the helium-3 bath was achieved by passing the off-balance signal from the phase sensitive detector into a difference amplifier. The output of this amplifier was then fed into a 500 Ω heater which was wound directly on the helium-3 vessel. With this arrangement the helium-3 bath temperature could be maintained constant to better than 5×10^{-5} degK for lengths of times normally required for accurate thermometer calibrations.

(*c*) *Measurement of the thermal conductivity*

The specimen and thermometer arrangement is shown in figure 2(*b*). The thermal conductivity was measured under steady state conditions with the well known two heater method (see, for example, Howling, Mendoza & Zimmerman 1955). The thermometers used were 10 Ω, $\frac{1}{10}$ W Allen–Bradley carbon resistors for the temperature range between 0·5 and 4·2 °K and carbon film resistors below 0·5 °K. The carbon film thermometers were painted on to an insulating layer of varnish that was baked on to the samples. The resistances of the thermometers were measured potentiometrically with measuring powers between 10^{-8} and 5×10^{-10} W depending on the temperature range. The thermometers were calibrated against the salt temperatures throughout the whole temperature range. The salt was in turn calibrated against the vapour pressure of the helium-4 bath between 1·5 and 4·2 °K by using the 1958 temperature scale. The susceptibility of the salt in the calibration range followed the Curie law within the experimental error and the shape correction for the salt pill used was sufficiently small so that it was usually neglected altogether. The mutual inductance was related to the temperature by the equation

$$1/T = M_0 + bM$$

and the parameters M_0 and b were determined by a least squares analysis of the calibration data. This equation was then used to calculate absolute temperatures below 1·5 °K. This procedure should be valid since it is known (Ambler & Hudson 1955) that cerium magnesium nitrate obeys the Curie law to temperatures well below 0·3 °K. Both the salt and the carbon thermometers were recalibrated every run. A three-constant logarithmic expression of the Clement–Quinnell type was used to obtain temperature deviation curves for each resistance, from which the absolute thermometer temperatures were computed. Most samples investigated were about 9 cm long and between 2 and 4 mm in diameter. Their thermal resistances at 1 °K were generally such that a heat flux of only 30 ergs/s was required to produce a temperature difference between the thermometers (normally 5 cm apart) of 0·1 degK. The temperature difference between the thermometers was never larger than 0·2 degK and usually about 0·04 degK at 0·4 °K.

Heater H_1 in figure 2 (*b*) was a single layer of no. 50 s.w.g. enamelled Eureka wire attached to a copper bobbin and had a resistance of about 5 kΩ. Joule heating in the electrical leads to the heater was therefore small compared to that in H_1. A simple potentiometer arrangement was used to measure the heater power

The overall accuracy of the thermal conductivity measurement was estimated to be about 1 % for most samples.

(*d*) *Electrical conductivity measurement*

The resistivity of the samples was measured by comparing the potential drop across a specimen with the drop across a substandard resistance of comparable magnitude connected in series with the sample. The null indicator was a Tinsley galvanometer amplifier and the potential difference across the samples, of about 100 μV, could easily be measured to 0·05 %.

TABLE 1. SAMPLE PREPARATION DETAILS

alloy no.	composition (at. %)		component materials: Ag	component materials: impurities	mode of preparation	annealing details: temp. (°C)	annealing details: time (h)	average grain size (mm)	remarks
1	Ag 95·13	Sb 4.85	5N filings	filings	boric acid flux melting under reduced pressure	670	70	0·1	—
2	Ag 94·47	Sb 5·52	3N powder (Johnson, Matthey)	filings (Hilger comp.)	boric acid flux melting under reduced pressure, second remelting	650	170	single crystal	—
3	Ag 98·00	Sb 2·00	1 in. rod 5N material (United Chem.)	filings (Hilger comp.)	induction furnace melting and shaping; slow cooling of melt	750	50	0·4	alumina crucible silica mould I
4	Ag 98	Sn 2	1 in. rod 5N material (United Chem.)	Sn Specpure (Johnson, Matthey)	as no. 3	820	60	0·3	
5	Ag 95	Sn 5	as no. 4	as no. 4	as no. 3	800	70	0·3	
6	Ag 99·2	Sb 0·8	6N shot (Light and Co.)	6N shot (Light and Co.)	as no. 3	850	70	7·5	
7	Ag 92	Sn 8	as no. 4	as no. 4	as no. 3 but rapid cooling of melt	750	90	0·5	silica crucible silica mould I
8	97 Ag	3 Sb	as no. 6	as no. 6	as no. 7	800	130	0·3	silica crucible silica mould II
C3	94 Cu	6 Ge	Cu 5N (Amer. Smelting and Refining Co.)	Ge 5N (Light and Co.)	as no. 7	850	65	—	graphite-lined silica crucible and mould I
C1	Cu–Sn		commercial material	rod	—	700	100	—	

4. Sample preparation

The main factors that determined the choice of the alloy system used are:

(*a*) Simplicity of the Fermi surface of the base metal.

(*b*) Range of α-phase solubility for impurities.

(*c*) Ease of preparation.

The monovalent noble metals seemed an obvious choice as base metal since their Fermi surface is quite well known from de Haas–van Alphen and magneto-acoustic measurements.

Silver was chosen for its lower melting point and since it is somewhat easier to produce homogeneous silver alloys than their copper counterparts. Furthermore, impurities dissolved in silver have a larger scattering cross-section than when dissolved in copper, so that for a given resistivity smaller quantities of impurities are required for silver than for copper (Blatt 1957).

The impurities chosen were antimony and tin. Both elements belong to the silver series and probably the only effect, apart from scattering, that the addition of impurities has is to increase the number of conduction electrons per atom. All alloys investigated were α-phase solid solutions.

Alloys no. 1 and no. 2 were prepared from powdered metal components which were mixed and then melted in silica tubes under forepump vacuum. The rest of the alloys were prepared from 99·999 % and 99·9999 % purity components in a vacuum induction furnace, where they were cast into cylindrical rods, which were then machined to the appropriate sizes. After machining all alloys were annealed in evacuated silica tubes. The preparation details and some alloy parameters are given in table 1.

5. Experimental results

(*a*) *The lattice thermal conductivity*

Silver base alloys

The thermal conductivity results for the alloys are presented in figures 3 to 7 and also in table 2. The lattice conductivity was computed by subtracting the electronic contribution ($K_e = (L_0/\rho_0)\, T$) from the measured total conductivity.

The overall thermal conductivity behaviour of the alloys can be summarized in the following way:

(i) Between 4·2 and 1·2 °K the conductivity can be described by an equation of the form

$$K = (L_0/\rho_0 + A)\, T + BT^2. \tag{9}$$

(ii) Below about 1·2 °K most alloys show a much more rapid decrease of the thermal conductivity with temperature than is suggested by the above equation.

The only silver base alloy which did not show this rapid decrease of the conductivity below 1 °K is alloy no. 4. This specimen was therefore remeasured in a number of runs with both Allen–Bradley and carbon-film thermometers being used. These results which are plotted in figure 4 establish firmly the long-term reproducibility of the apparatus as well as the absence of any significant deviation from the behaviour given by equation (9). (For alloy no. 1 in figure 3 and alloy no. 4 in figure 4 different symbols for the experimental points represent data for different runs.)

In order to investigate the effect of dislocations on the lattice conductivity of these alloys, sample no. 5 was strained axially at room temperature by about 3·6% and its conductivity was then remeasured. The results for this alloy 5*A* are shown in figure 5 and a comparison of these results with those for the unstrained specimen no. 5 shows that the temperature variation of the conductivity was essentially unaffected by the introduction of dislocations.

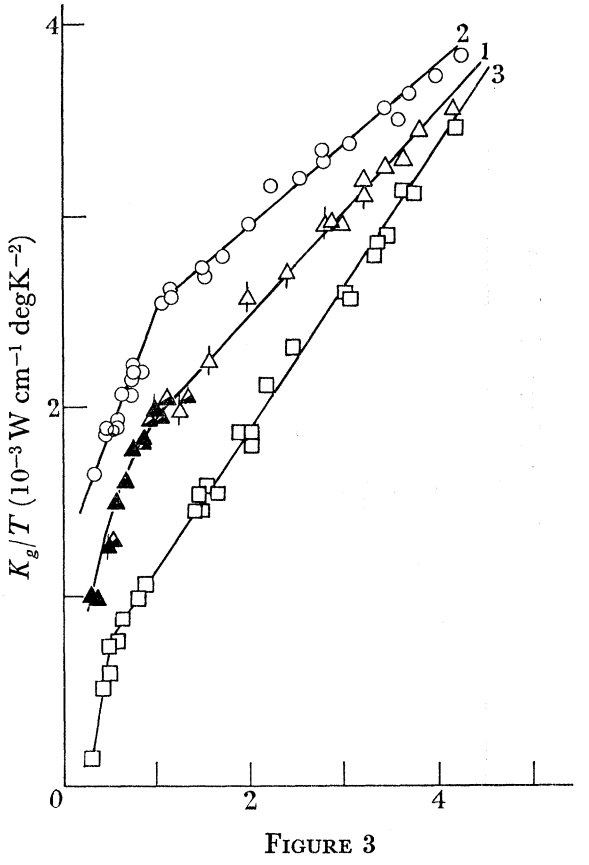

FIGURE 3

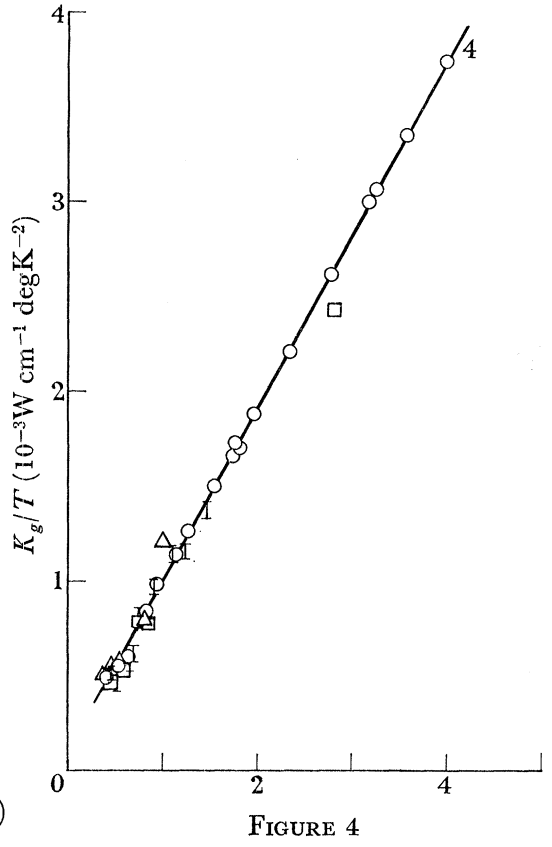

FIGURE 4

FIGURE 3. Lattice conductivities for samples 1, 2 and 3 divided by the absolute temperature as function of the absolute temperature.

FIGURE 4. Lattice conductivity of sample 4 divided by the absolute temperature as function of the absolute temperature.

TABLE 2. A LIST OF VARIOUS ALLOY PARAMETERS

alloy no.	ρ_0 ($\mu\Omega$ cm)	$q_l l$ (at 1 °K)	$q_t l$ (at 1 °K)	δ/λ_t (at 1 °K)	phonon m.f.p. at 1 °K (cm)	L_0/ρ_0 (Wcm^{-1} degK^{-2})	$10^3 A$ (Wcm^{-1} degK^{-2})	$10^4 B$ (Wcm^{-1} degK^{-3})
1	30·8	0·16	0·36	206	$2{\cdot}3\times10^{-3}$	$0{\cdot}795\times10^{-3}$	$1{\cdot}41\pm0{\cdot}03$	$5{\cdot}43\pm0{\cdot}25$
2	36·08	0·14	0·32	221	2·7	$0{\cdot}679\times10^{-3}$	$2{\cdot}13\pm0{\cdot}02$	$4{\cdot}33\pm0{\cdot}3$
3	14·55	0·35	0·79	141	1·27	$1{\cdot}68\times10^{-3}$	$0{\cdot}4\pm0{\cdot}04$	$7{\cdot}7\pm0{\cdot}4$
4	8·136	0·62	1·4	105	1·13	$3{\cdot}01\times10^{-3}$	$0{\cdot}08\pm0{\cdot}02$	$9{\cdot}1\pm0{\cdot}25$
5	17·95	0·28	0·63	158	1·61	$1{\cdot}37\times10^{-3}$	$0{\cdot}96\pm0{\cdot}05$	$5{\cdot}5\pm0{\cdot}2$
6	5·05	1·0	2·26	83	1·0	$4{\cdot}85\times10^{-3}$	$0{\cdot}05\pm0{\cdot}1$	$1{\cdot}12\pm0{\cdot}03$
7	26·72	0·19	0·43	186	2·06	$0{\cdot}918\times10^{-3}$	$1{\cdot}31\pm0{\cdot}03$	$5{\cdot}15\pm0{\cdot}2$
8	19·9	0·25	0·57	166	1·81	$1{\cdot}23\times10^{-3}$	$1{\cdot}04\pm0{\cdot}02$	$5{\cdot}5\pm0{\cdot}3$
C_3	17·99	0·28	0·64	153	3·6	$1{\cdot}36\times10^{-3}$	$1{\cdot}01\pm0{\cdot}03$	$2{\cdot}45\pm0{\cdot}15$
C_2	$1{\cdot}885\times10^{-2}$	—	—	—	—	1·30	—	—
C_1	7·08	—	—	—	—	$3{\cdot}46\times10^{-3}$	—	—

The Cu base samples

The results for two copper alloys C_1 and C_3 are shown in table 2 and figure 7. The Cu-Ge alloy C_3 follows the behaviour of the silver alloys quite closely, while the behaviour of sample C_1 like the silver sample no. 4 seems to follow equation (9) down to the lowest

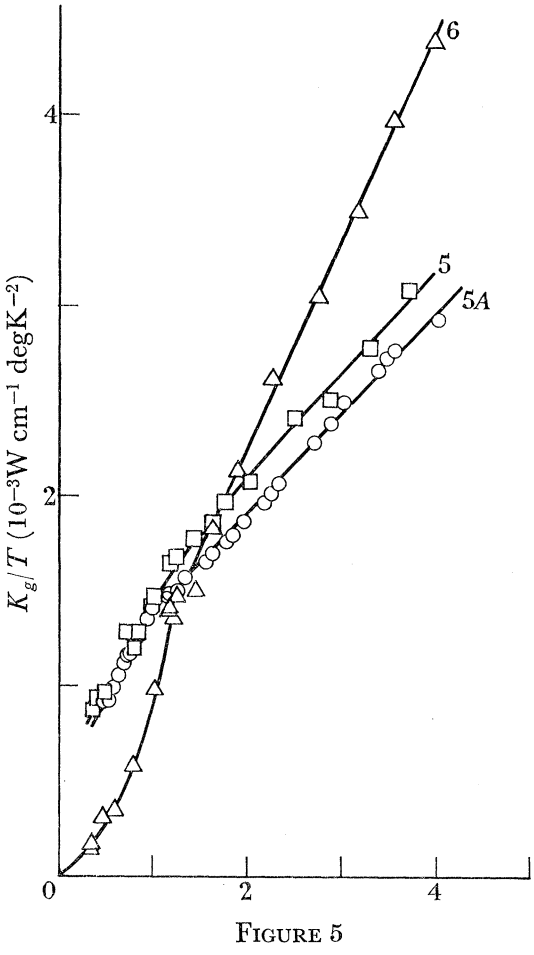

FIGURE 5

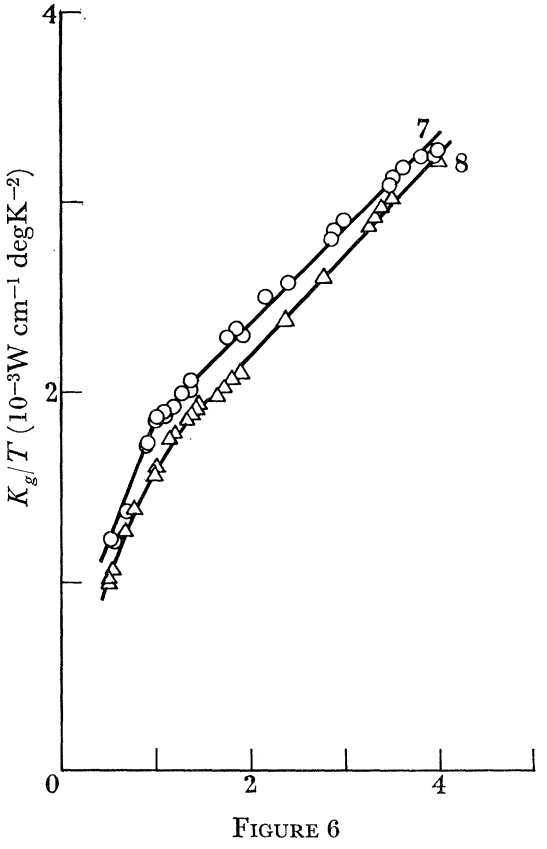

FIGURE 6

FIGURE 5. Lattice conductivities for samples 5, 5*A*, and 6 divided by T as function of T.

FIGURE 6. Lattice conductivity for samples 7 and 8 divided by T as function of T.

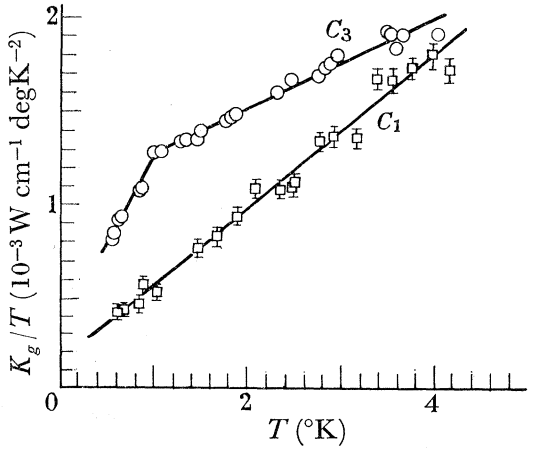

FIGURE 7. Lattice conductivity for samples C_1, and C_3 divided by T as function of T.

temperatures. The results on C_1 are an early set of data and the accuracy of the measurements is not as high as for the other samples. The absence of any significant low-temperature anomally seems quite definitely established, however.

In the course of these experiments on the alloys an unannealed length of bare no. 27 s.w.g. copper wire (sample C_2) was also investigated for its thermal and electrical properties and the results are shown in figure 8. The specimen had a resistance ratio of about 85 so that the lattice contribution to the total heat current should be negligible.

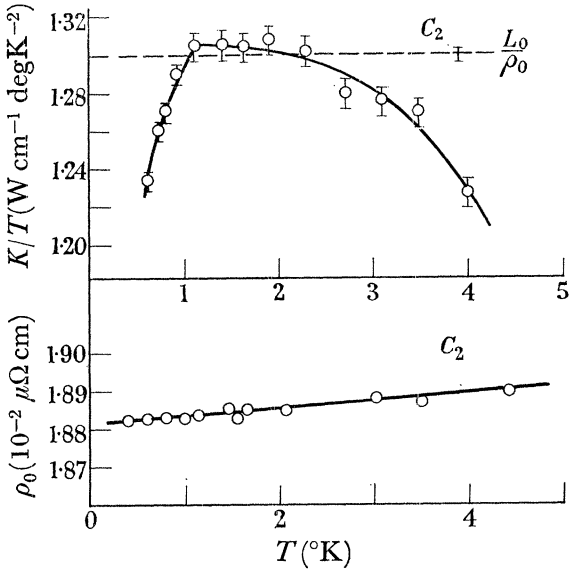

FIGURE 8. Temperature variation of the thermal and electrical conductivity of sample C_2.

(*b*) *The electrical resistivity results*

These results are summarized in figures 9 and 10 and table 2. The resistance of most samples was constant to within 1% in the liquid helium range of temperatures. Some samples such as alloy no. 3 and no. 5 had a negative temperature coefficient of resistance. The results for alloy no. 3 are particularly puzzling. The shape of the resistance step was quite reproducible and as figure 9 shows, temperature cycling of the sample had no effect on the resistivity (absence of any hysteresis effects). The positive temperature coefficient of resistance shown by some samples near 4 °K can most likely be attributed to superconducting films near the potential probes since tin-indium solder was used for the attachment of the potential leads in all cases except alloy 5*A*. (The positive temperature coefficient of resistance shown by copper sample C_2 cannot be explained this way, however, since this sample was much longer than the alloy specimens.) Results for a series of control samples containing different amounts of antimony showed that the anomalous behaviour of alloy no. 3 did not seem to depend on the antimony content. The control samples that had a similar antimony concentration to alloy no. 3 did not show this resistivity step while a similar step was again observed in a silver-2·4% antimony alloy. The origin of this resistance anomaly is not clear. In the computation of the electronic thermal conductivity the average value of the low temperature resistivity was used.

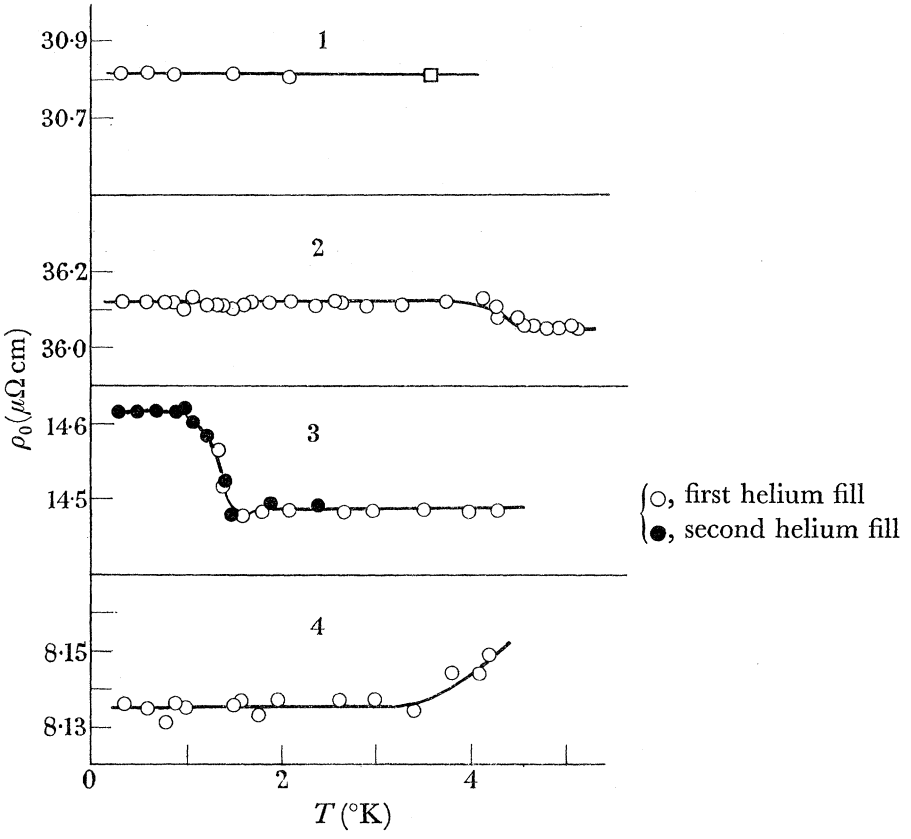

FIGURE 9. Temperature variation of the electrical resistivity of samples 1, 2, 3, and 4.

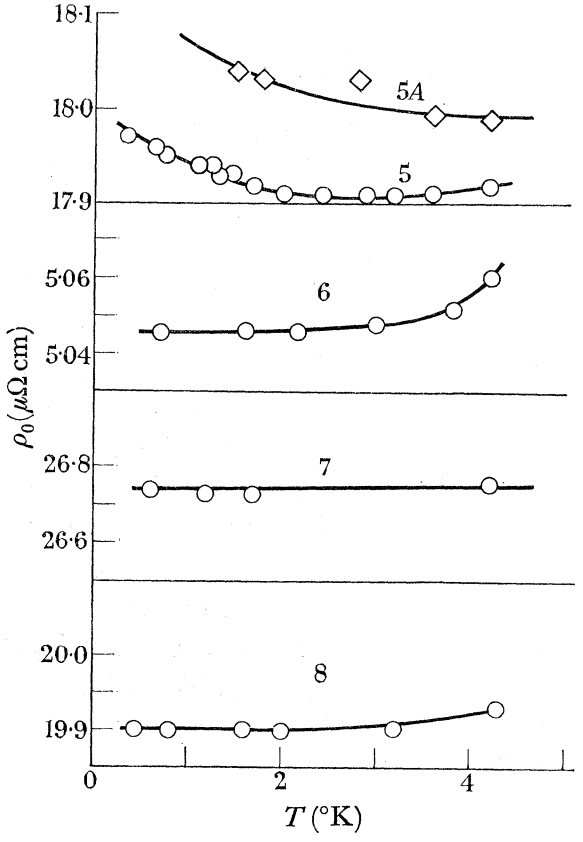

FIGURE 10. Temperature variation of the electrical resistivity of samples 5, 5*A*, 6, 7, and 8.

6. Comparison of the results with the theoretical models

In view of the unexpected low-temperature behaviour of these alloys a comparison of the experimental results with the theory developed in § 2 will be restricted to the temperature range between 1·2 and 4 °K. In figure 11 are shown the coefficients A in equation (9) which were obtained by extrapolating the results in this temperature range to zero temperature. The agreement with Zimmerman's (1959) results is fairly good. The dashed line in figure 11 is the theoretical variation of A for the free electron model of a metal.

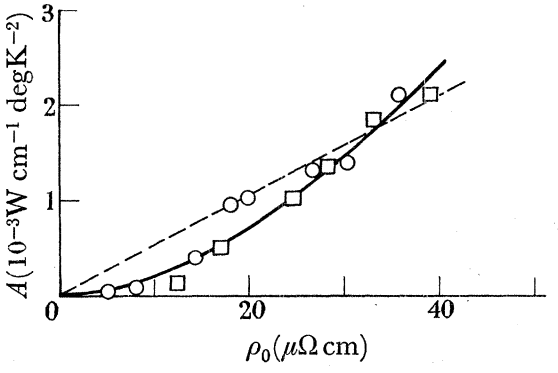

Figure 11. Residual resistivity variation of the linear lattice term A in the expression $Kg = AT + BT^2$. ------, Theoretical; ○, this work; □, Zimmerman (1959).

Above a residual resistivity of about 20 $\mu\Omega$ cm the agreement is fair while consistently lower values are obtained for the more dilute alloys. This fact is perhaps not too surprising since the conductivity curves in figures 3 to 7 should level off at the lowest temperatures so that an extrapolation of the results in the liquid helium range of temperatures would tend to underestimate the coefficients A.

A more direct comparison between experiment and theory is possible if we plot the results directly as a reduced conductivity plot such as figure 1. This is done in figure 12 for all silver alloys and the whole temperature range covered. The experimental points have been omitted for the sake of clarity. The theoretical curves shown in figure 1 for the total lattice conductivity have also been plotted on figure 12. The agreement with the theoretical plots for temperatures above 1 °K and for residual resistivities above 5 $\mu\Omega$ cm is fairly good in view of the various simplifying assumptions that were made in the derivation of the theoretical curves.

Of particular significance in this comparison is the straightness between 4 and 1 °K in the curves for the alloy samples. Furthermore, extrapolation of the alloy results for the purer samples to higher temperatures (larger T/ρ_0 values) results in progressively increasing deviations between the experimental curves and the theoretical curve 1. This general behaviour can be understood at least qualitatively as pointed out in § 2 if the free electron model is abandoned. The shear wave attenuation could then be expected to have a very similar frequency dependence as the longitudinal branches. The expected temperature variations would therefore be the same for the two polarization branches and the total lattice conductivity would instead vary as T^2 throughout the greater part of the temperature range.

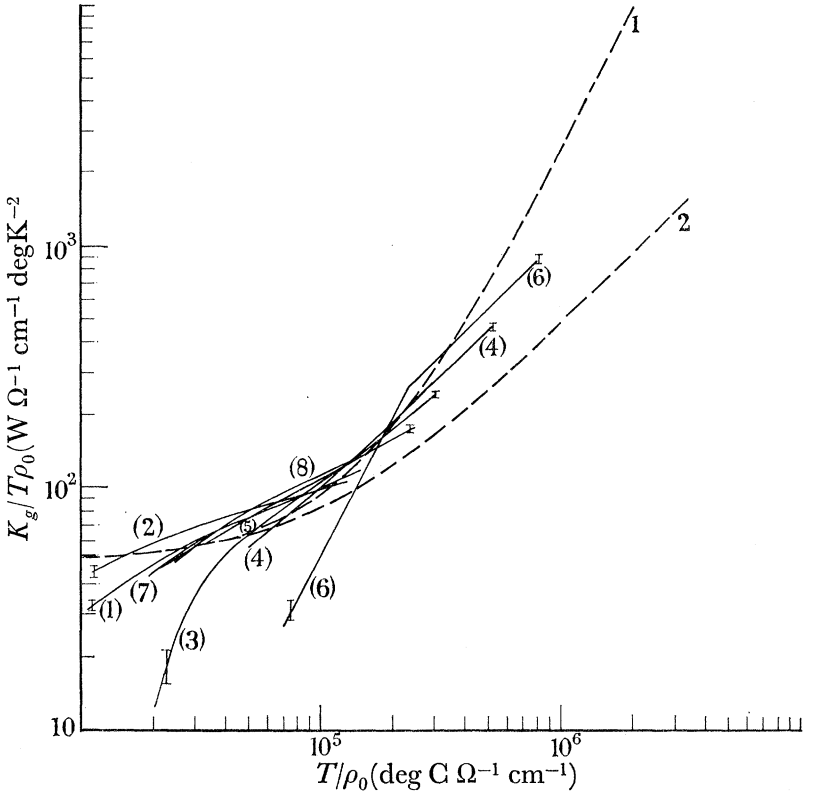

FIGURE 12. Comparison of the lattice thermal conductivity results for the silver alloys with the theoretical curves of figure 1.

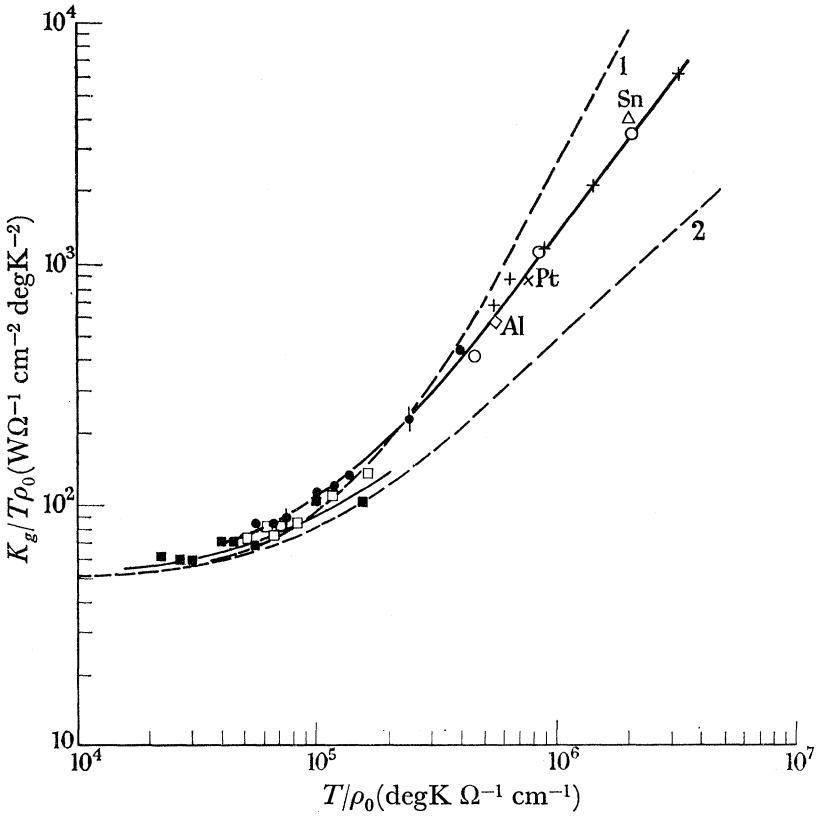

+, Ag–Cd; ○, Ag–Pd; (Tainsh & White 1962).
□, Ag–Sb (Zimmerman).
●, Ag–Sb; ⧫, Ag–Sn (this work).
■, this work, T = 0·8 °K.
} T = 2 °K

FIGURE 13. Comparison of the theoretical lattice conductivity curves with the alloy results for T = 2 °K and 0·8 °K.

It is interesting to plot the data in a different way. In figure 13 the lattice conductivities of the alloy samples are compared at a few fixed temperatures. Some of the results of other authors have also been included. Most alloy points for a given temperature lie on a universal curve irrespective of the quantity and type of solute. The curvature effect, that is, the gradual weakening of the electron-phonon interaction seems therefore well established. The quantitative agreement cannot be expected to be much better than 5 to 10% since the alloy parameters, such as sound velocities and Debye temperatures, are subject to variation on alloying as experiments by Rayne (1957–58) on copper-zinc and copper-germanium alloys have shown. The reason for the somewhat closer fit of the experimental results with the theoretical curve 1 when different samples are compared at a fixed temperature is not clear at present and is subject to further investigation.

From the discussion in § 2 as well as from figure 12 it seems likely that the lattice conductivity of the alloys in the region $ql \gg 1$ is dominated by the transverse polarization branches. It is not possible, however, to make any more quantitative predictions about the relative contributions of the longitudinal and transverse modes to the heat transport until the calculations of § 2 are carried out for a more realistic Fermi surface for silver.

The low-temperature thermal conductivity

In order to explain the sharp increase in the thermal resistance of most of the samples investigated it must be decided whether the conduction electrons or the lattice vibrations are responsible for the observed effect. The results on the copper specimen of figure 8 seem to suggest that all the observed anomalies must be attributed to the conduction electrons. This is not necessarily so, however, and various aspects of the lattice conductivity curves of figures 3 to 7 suggest that at least part of the effect is attributable to the phonons. The shape of the anomaly in the alloys is such that it seems as if the total conductivity is heading towards the electronic value. This is particularly well demonstrated by alloys nos. 2, 7 and 6. Furthermore, if the electrons alone are responsible for the deviation then their contribution to the heat current would have virtually ceased near 0·2 °K for some of the alloys of highest resistivity. This seems rather improbable. It is therefore reasonable to look for extra phonon scattering mechanisms which become important at the lowest temperatures. (A phonon mechanism would also be consistent with the observed absence of a similar anomaly in the electrical conductivity of most alloys, although inelastic electron scattering could give rise to a similar behaviour.)

Of the many possible phonon scattering mechanisms two have been studied in detail by calculating their effects on the theoretical conductivity curves of § 2. Point scattering and phonon-phonon interactions are probably quite negligible in the temperature range below about 2 °K. In the long wavelength limit phonon impurity scattering is of the Rayleigh type, that is, the scattering cross-section varies as ω^4. The mass difference scattering can be computed with Klemens's (1955) formula and turns out to be negligible for the temperature range of this experiment. That phonon point scattering is most likely negligible is also evident from the work of Toxen (1961) on the thermal conductivity of germanium-silicon alloys.

The only direct evidence that multi-phonon processes are negligible at liquid helium temperatures is obtained from the observation by Bömmel & Dransfeld (1960) that the

PHILOSOPHICAL TRANSACTIONS OF THE ROYAL SOCIETY A MATHEMATICAL, PHYSICAL & ENGINEERING SCIENCES

ultrasonic attenuation in quartz becomes temperature-independent below 10 °K. It is not directly obvious, however, that the results for quartz are also valid for electrical conductors.

For the calculation of the extra thermal resistance that is caused by phonon-dislocation and phonon-boundary scattering the reciprocals of the phonon mean free paths for electron-phonon scattering and electron dislocation or boundary scattering were added and substituted for $1/\Lambda_{\text{eff.}}$ in equation (8). The mean free path for electron-phonon scattering was assumed to be given by expressions (5) and (6). The integrals were evaluated numerically as before. Some of the results are shown in figures 14 and 15. Figure 14 shows the effect of

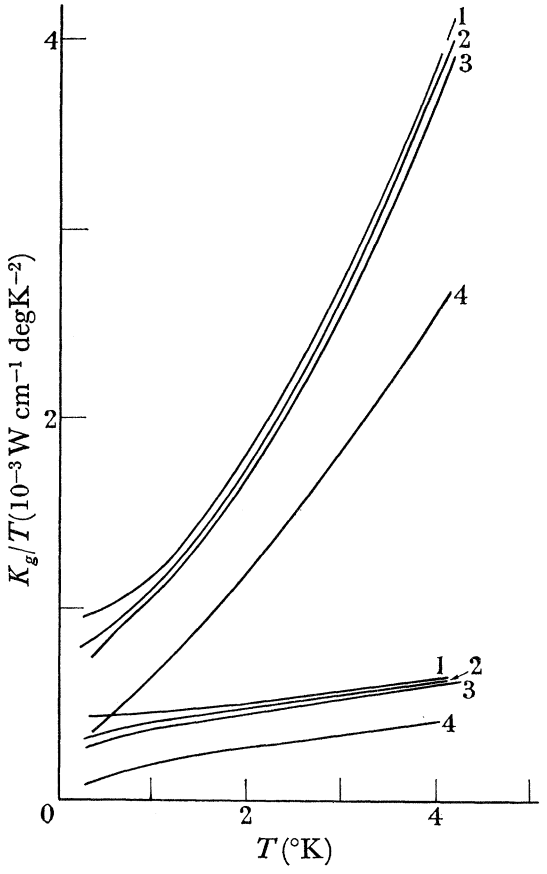

Top curves, total lattice conductivity; bottom curves, longitudinal modes only.

curve	1	2	3	4
N (lines/cm^2)	0	5×10^9	10^{10}	10^{11}

FIGURE 14. Effect of dislocations on the theoretical lattice conductivity curves. The computations were carried out for a residual resistivity of 18 $\mu\Omega$ cm.

dislocations on the lattice conductivity of an alloy with a residual resistivity of 18 $\mu\Omega$cm. In the calculation the phonon mean free path for dislocation scattering was assumed to be that derived by Klemens (1955)

$$\Lambda_D = \frac{v_s}{6\times10^{-2}b^2\gamma^2\omega Nf},$$

where v_s is the sound velocity, b the Burgers vector, γ the Grüneisen constant, ω the phonon frequency and f (which has a value of about 5) ensures that the dislocation densities as derived from thermal measurements agree with those derived from stored energy release

data and electron micrograph studies. N is the dislocation density and was an adjustable parameter. The interesting aspect of these curves is the almost parallel displacement of the curves to lower conductivity values as the dislocation density increases. The shape of the curves is only significantly affected at the lowest temperatures, although no major changes seem to be taking place after a dislocation density of about 5×10^9 lines/cm^2.

This theoretically derived effect of dislocations on the lattice conductivity is very similar to the observed change in the lattice conductivity of alloy no. 5 after it was axially strained by 3·6%. That is, the curve for alloy 5A in figure 5 is almost parallel to that of the unstrained sample while the extrapolated intercept has decreased by about 15%. If we assume that all of the extra thermal resistance in the strained sample is due to dislocations and that alloy no. 5 was free from dislocations then the results of the theoretical calculations in figure 14 would indicate that the dislocation density that was introduced in the straining operation was of the order of 10^{10} lines/cm^2. This figure seemes reasonable and is of the same order of magnitude as the dislocation densities reported by Lomer & Rosenberg (1959) for copper-zinc alloys strained by similar amounts.

The strain experiment shows that static dislocations have a small effect on the overall lattice conductivity of the alloys above 1 °K and is further evidence that the observed electrical resistivity variation of the lattice thermal conductivity is not connected with dislocations as was suggested by Klemens & Kemp (1960). Other evidence for this was obtained by Lomer & Rosenberg (1959) as well as by Lindenfeld & Pennebaker (1961) from direct dislocation counts in alloy foils with an electron microscope.

The addition of dislocations to alloy no. 5 had very little effect on the general shape of the low temperature end of the conductivity curve. The onset of the anomalous behaviour is probably shifted to a somewhat lower temperature although this cannot be determined with certainty. At still lower temperatures than those investigated the extra phonon scattering that seems to give rise to the anomalous behaviour will most probably dominate over phonon dislocation scattering so that the two curves can be expected to merge into each other.

In the case of boundary scattering of phonons the phonon mean free path was assumed to be constant and limited by internal boundaries of an unspecified origin. The effective phonon mean free path in this case was taken to be

$$1/\Lambda_{\text{eff.}} = 1/\Lambda_{\text{e.p.}} + 1/b,$$

where b is some boundary parameter. The results for the numerical calculations for this case are shown in figure 15, for $b = 1$, 0·1, 0·01 and 0·001 cm. The same general behaviour above about 1 °K as for the dislocation scattering is noticeable. The curves get displaced downwards as the boundary parameter decreases with very little change in shape. The downward curvature of the curves below 1 °K is much more pronounced for boundary scattering, however. This is what one would expect since boundary scattering gives rise to a stronger temperature dependence (T^3) of the conductivity than dislocation scattering. The corresponding experimental curve for this resistivity value is that for alloy no. 1 and is also plotted on figure 15. In that sample—as in most other specimens—the decrease in the conductivity below about 1 °K is much more rapid than is shown by the theoretical curves. This would suggest that a phonon scattering mechanism which gives rise to an even

PHILOSOPHICAL TRANSACTIONS OF THE ROYAL SOCIETY A MATHEMATICAL, PHYSICAL & ENGINEERING SCIENCES

stronger temperature dependence of K_g than T^3 is required to explain the experimental results.

It was originally thought that phonon scattering from mobile dislocations might be responsible for the observed effect. As was shown by Granato (1958) this type of scattering would give rise to a lattice conductivity varying as $T^{3\cdot8}$. A numerical calculation along similar lines as for the previous cases was carried out for this scattering mechanism and it is interesting to note that dislocation densities (mobile dislocations) as low as 10^6 lines/cm^2 turned out to be sufficient for obliterating the expected upward curvature in the conductivity curves for the alloys. The theoretical model which was used by Granato to calculate the lattice conductivity was very crude, however, and the present analysis did not go

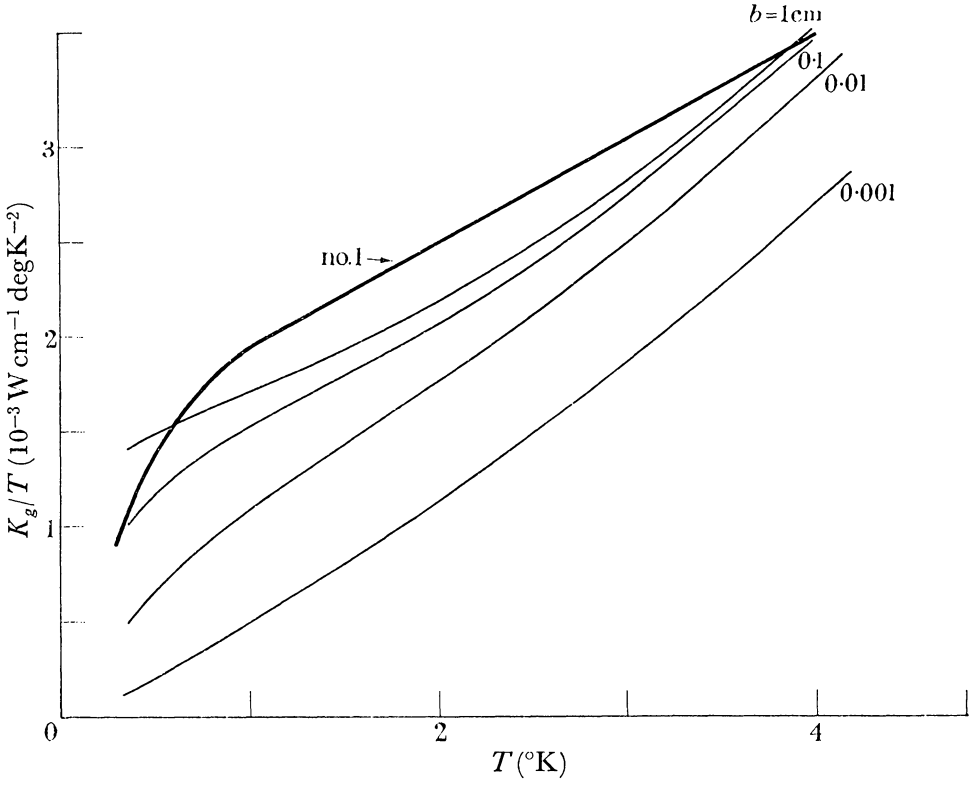

FIGURE 15. Effect of boundary scattering on the theoretical lattice conductivity curves. The calculations were done for $\rho_0 = 30{\cdot}8\ \mu\Omega$ cm. The thick curve gives the experimental results for alloy no. 1.

beyond it. It is also unlikely for a dislocation in an alloy to actually move or vibrate in the presence of a low-temperature phonon since the natural frequency of a mode of vibration of a dislocation line would be greatly increased by impurity pinning so that phonons with frequencies that are much larger than the average phonon frequencies at low temperatures would be required to move a dislocation.

The theoretical analysis of the effect of extra phonon scatterers on the lattice thermal conductivity of high resistivity alloys has shown that an additional scattering mechanism will reduce the lattice conductivity of an alloy such that the general shape of the conductivity curves is only weakly affected in the temperature range above 1 °K. This result is probably independent of the details of the assumed model for the Fermi surface.

Below 1 °K phonon scattering from dislocations and internal or grain boundaries can dominate the phonon-electron scattering since the latter should approach a linear temperature-dependence as soon as $ql < 1$ for most phonons. From a comparison of the experimental results with the theoretical curves of figures 14 and 15 it is not possible to determine the exact temperature dependence of the additional phonon scattering mechanisms that seem to be active in these alloys. It can at best be said that the scattering mechanism must give rise to a conductivity which varies as the third or higher power in the temperature.

There is one feature of these results which cannot be explained by postulating an additional phonon scatterer which is active throughout the whole temperature range. This is the fairly sharp change in the lattice conductivity near 1 °K shown by sample no. 6 and possibly also nos. 5, 5A, and 7. In these alloys the onset of the anomalous behaviour is much more rapid than is shown by any of the theoretical curves and seems to point to a form of phase transition that is taking place. To the knowledge of the author no anomalous behaviour of the specific heat of these alloy systems has been reported. The results for alloy no. 6 are particularly puzzling since the lattice conductivity seems to be changing almost discontinuously at 1·2 °K from a T^2 to a T^3 behaviour. This would suggest that the phonon mean free path for this sample is constant ($\sim 10\,\mu$m) below 1·2 °K. This is surprising since as tables 1 and 2 show alloy no. 6 had the shortest average phonon mean free path and the largest grain size so that phonon grain boundary scattering cannot be responsible for the effect. The fact that the single crystal alloy no. 2 behaved in the same way as the other polycrystalline samples seems to be further evidence for the negligible effect of grain boundaries on the lattice conductivity.

It was pointed out by Lindenfeld and McLaren (private communication) who observed similar low-temperature anomalies in a few copper alloys that the phonon mean free path in the alloys might be limited by subgrain boundaries, that is, the mosaic structure. The scattering cross-section for phonons from such low-angle grain boundaries has been worked out by Klemens (1955) and was found to be temperature independent. Although the scattering cross-section from low-angle grain boundaries turned out to be much smaller than for grain boundaries proper, the much larger number of subgrain boundaries per unit volume could possibly, however, make a substantial contribution to the lattice thermal resistance. The silver samples were not analysed for their mosaic structure so that it was not possible to obtain a realistic estimate of their effect on the alloy thermal conductivity.

This type of scattering mechanism cannot be the only one active, however, since as pointed out before the thermal resistance of some alloys increases much more rapidly near 1 °K than can be accounted for with a temperature independent boundary scattering term.

It is of course possible that a similar breakdown of the Wiedemann–Franz law as observed in the copper cample C_2 in figure 8 is taking place in the alloys. This would have only a small effect on the conductivities of the high resistivity alloys but could make a measurable contribution in a dilute alloy such as no. 6.

The breakdown of the Wiedemann–Franz law in the copper sample C_2 is somewhat similar to that observed by Mendelssohn & Davey (1963) in a number of pure materials. No explanation for this breakdown has been given yet.

The results for the copper-germanium alloy C_3 seem to suggest that the anomalous thermal conductivity behaviour is a general property of these noble metal alloys and not a peculiarity of the silver system.

7. Summary

The thermal and electrical conductivity measurements on eight silver and two copper base alloys confirm the results of Zimmerman (1959) and Lindenfeld & Pennebaker (1962) and demonstrate the important part that the transverse polarization branches play in the lattice thermal conduction of metals. Even though the gradual weakening of the electron-phonon interaction could not be observed directly by studying a given alloy sample, the overall alloy behaviour between 1 and 4 °K seems well accounted for by the semi-classical theories on the electron-phonon interaction.

Below about 1 °K the thermal conductivity of most alloys decreased much more rapidly than one would have expected from the theoretical models. In an attempt to understand the observed behaviour, phonon scattering mechanisms other than the electron-phonon interaction were postulated and the effects of dislocations and boundary scattering on the lattice conductivity were studied in detail. It turned out that the theoretically predicted change-over of the lattice conductivity to a linear temperature dependence is very sensitive at the lowest temperatures to the number of dislocations present and a dislocation density of 10^9 lines/cm^2 could easily linearize the theoretical curves of K_g/T against T. Since the dislocation density in well annealed alloys is most likely much lower than this value no serious difficulty should arise from this scattering mechanism.

Phonon-boundary scattering can be even more effective in rendering the weakening of the electron-phonon interaction unobservable at the lowest temperatures although it should be possible to overcome this difficulty by studying samples consisting of only a few large grains which are several millimetres in diameter. There is the possibility that in the alloys investigated the phonon mean free path was substantially affected by the mosaic structure although this cannot be confirmed at present. Further investigations which are hoped to elucidate the cause of the low temperature anomaly are in progress.

It is a great pleasure to thank Professor A. B. Pippard, F.R.S., for his assistance, interest and encouragement throughout the course of this work. Many helpful discussions with other members of the Mond Laboratory and in particular Dr B. Abraham are also gratefully acknowledged. The work was carried out with financial assistance from the Department of Scientific and Industrial Research.

References

Adkins, J. C. 1961 *J. Sci. Instrum.* **38**, 305.
Ambler, E. & Hudson, R. P. 1955 *Rep. Progr. Phys.* **18**, 251.
Blatt, F. J. 1957 *Phys. Rev.* **108**, 285.
Bömmel, H. E. & Dransfeld, K. 1960 *Phys. Rev.* **117**, 1245.
Callaway, J. 1959 *Phys. Rev.* **113**, 1046.
Chester, G. V. & Thellung, A. 1961 *Proc. Phys. Soc.* **77**, 1005.
Granato, A. 1958 *Phys. Rev.* **111**, 740.
Howling, D. H., Mendoza, E. & Zimmerman, J. E. 1955 *Proc. Roy. Soc.* A, **229**, 86.
Klemens, P. G. 1955 *Proc. Phys. Soc.* A, **68**, 1113.

PHILOSOPHICAL TRANSACTIONS OF THE ROYAL SOCIETY A MATHEMATICAL, PHYSICAL & ENGINEERING SCIENCES

Klemens, P. G. 1958 *Solid State Phys.* vol. 7, p. 1. New York: Academic Press.
Klemens, P. G. & Kemp, W. R. G. 1960 *Aust. J. Phys.* **13**, 247.
Lindenfeld, P. & Pennebaker, W. B. 1961 *Proc. Int. Conf. on Low Temp. Phys.* University of Toronto Press.
Lindenfeld, P. & Pennebaker, W. B. 1962 *Phys. Rev.* **127**, 1881.
Lomer, J. N. & Rosenberg, H. M. 1959 *Phil. Mag.* **4**, 467.
Mendelssohn, K. & Davey, G. 1963 *Phys. Lett.* **7**, 183.
Olsen, T. 1960 *J. Phys. Chem. Sol.* **12**, 167.
Pippard, A. B. 1957 *J. Phys. Chem. Sol.* **3**, 175.
Pippard, A. B. 1960 *Proc. Roy. Soc.* A, **257**, 165.
Pippard, A. B. 1962 *Low temperature physics.* New York: Gordon and Breach.
Rayne, J. A. 1957 *Phys. Rev.* **108**, 22.
Rayne, J. A. 1958 *Phys. Rev.* **110**, 606.
Seidel, G. & Keesom, P. H. 1958 *Rev. Sci. Instrum.* **29**, 606.
Tainsh, R. J. & White, G. K. 1962 *J. Phys. Chem. Sol.* **23**, 1329.
Toxen, A. 1961 *Phys. Rev.* **122**, 450.
Zimmerman, J. E. 1959 *J. Phys. Chem. Sol.* 11, 299.

PHILOSOPHICAL TRANSACTIONS OF THE ROYAL SOCIETY A MATHEMATICAL, PHYSICAL & ENGINEERING SCIENCES